Australian Government
Geoscience Australia

Velocity Analysis and Depth Conversion in the Offshore Northern Perth Basin, Australia

Stephen Johnston and Alexey Goncharov

Record
2012/33

GeoCat #
73001

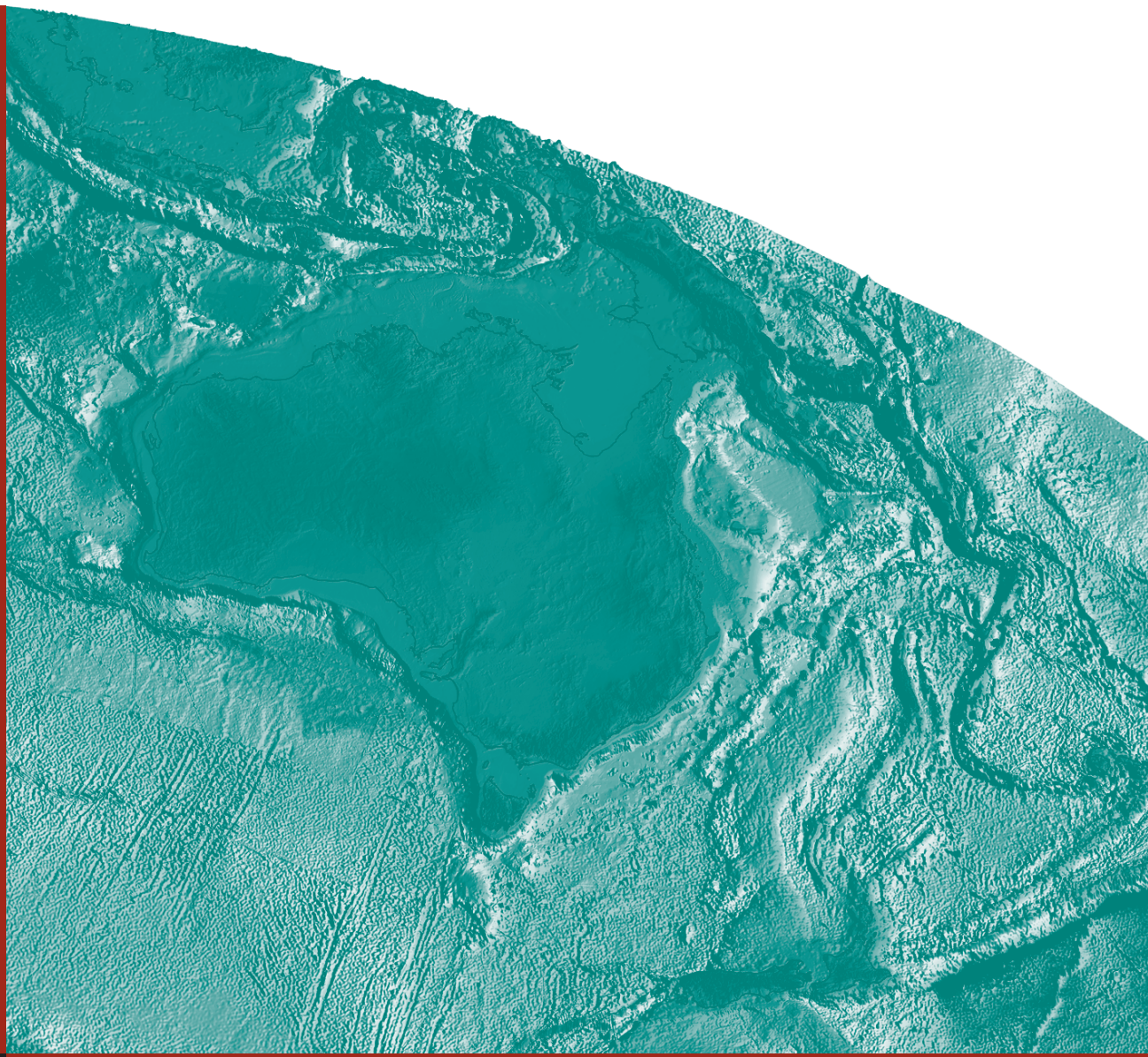

Velocity Analysis and Depth Conversion in the Offshore Northern Perth Basin, Australia

GEOSCIENCE AUSTRALIA
RECORD 2012/33

by

Stephen Johnston and Alexey Goncharov

Australian Government
Geoscience Australia

Energy Division, Geoscience Australia, GPO Box 378, Canberra, ACT 2601.

Department of Resources, Energy and Tourism
Minister for Resources and Energy: The Hon. Martin Ferguson, AM MP
Secretary: Mr Drew Clarke

Geoscience Australia
Chief Executive Officer: Dr Chris Pigram

© Commonwealth of Australia (Geoscience Australia) 2012

With the exception of the Commonwealth Coat of Arms and where otherwise noted, all material in this publication is provided under a Creative Commons Attribution 3.0 Australia Licence (http://creativecommons.org/licenses/by/3.0/au/)

Geoscience Australia has tried to make the information in this product as accurate as possible. However, it does not guarantee that the information is totally accurate or complete. Therefore, you should not solely rely on this information when making a commercial decision.

ISSN 1448-2177
ISBN 0-642-978-1-922103-10-9

GeoCat # 73001

Bibliographic reference: Johnston, S. and Goncharov, A., 2012. Velocity Analysis and Depth Conversion in the Offshore Northern Perth Basin, Australia. Geoscience Australia Recod, 2012/33, 32p.

Contents

Executive Summary

The Perth Basin is an elongate sedimentary basin, located along the southwestern margin of Australia. The offshore part of the basin is prospective for petroleum resources, but is relatively under-explored, and the nature of the sediment-basement contact is relatively unknown due to a high degree of structuring and deep basement depth inhibiting seismic imaging. Accurate depth conversion of seismic interpretation is vital for use as constraints in gravity modelling and in other basin modelling tasks, but depth conversion requires good quality seismic velocity information. The number and distribution of wells with velocity information in the offshore northern Perth Basin is poor, but there exists a large amount of seismic stacking velocities. Seismic stacking velocities are an outcome of seismic processing and are thus not a direct measurement of the speed of sound in rocks. To improve the quality of stacking velocities we propose a methodology to calibrate stacking velocities against well velocities, which is as follows:

1. Check each velocity dataset for errors
2. Modify the datum of each dataset to the sea floor
3. Convert all datasets to TWT and depth domain
4. Resample all velocity datasets to the same depth intervals
5. Cross plot stacking velocity depths near a well site with corresponding well depths
6. Fit a linear polynomial to this cross-plot (higher order polynomials were tried also), and determine calibration coefficient from the gradient of the polynomial.
7. Grid calibration coefficients
8. Multiply depths derived from stacking velocities by calibration coefficient grid

An assessment of depth conversion errors relative to wells shows that this methodology improves depth conversion results to within ±50m; this depth uncertainty translates into a gravity anomaly error of about ±20 gu, which is acceptable for regional scale gravity modelling.

Introduction

Depth conversion of time based seismic interpretations is required for a variety of basin analysis tasks, in particular for providing constraints on gravity modelling. In addition to depth conversion, seismic velocity information is an integral part of offshore geological studies as it allows velocity models of the basin to be built which can be used to predict lithology and fluid content. In the northern Perth Basin, seismic velocity information is available from two sources: exploration and production wells, and stacking of reflection seismic data.

The northern Perth Basin is located onshore and offshore on the southwestern margin of Australia. The initial basin forming event took place during the Paleozoic to Mesozoic within an obliquely oriented extensional rift system (Quaife et al., 1994; Mory and Iasky, 1996; Norvick, 2004). It has proven petroleum potential (e.g. Jones et al., 2011), but is under-explored.

Seismic velocities from wells are measured by sonic log tools or check shot surveys and are a direct measurement of the seismic velocity of the subsurface immediately around the borehole. Stacking velocities are a product of processing seismic reflection data and are not direct measurements of the physical properties that define seismic velocity (e.g. Al-Chalabi, 1974). In the offshore northern Perth Basin, only 19 wells with adequate velocity information exist over the 172,300 km^2 area of the basin (Figure 1). This means that there is only a small amount of direct seismic velocity measurements. In contrast, seismic reflection data cover the entire region with fairly close spacing (Figure 1), so stacking velocities are widely available. The end result is that there are far more indirect measurements of seismic velocities than direct measurements. While stacking velocities are routinely used for the depth conversion of seismic interpretation (e.g. Reilly, 1993; Etris et al., 2001; Veeken et al., 2005), the calibration of stacking velocities against borehole velocity measurements would allow the widespread stacking velocities to be used to create a more constrained velocity model of the northern Perth Basin. This leads to the question: is there a way to improve the quality of the stacking velocities in order to create a basin-wide velocity model for use in depth conversion of reflection seismic data? This study aimed to create an easily implemented workflow for calibrating seismic stacking velocities against well velocities for use in depth conversion of seismic interpretation. The quality of the depth conversion needed to be such that the error in calculated depths would satisfy certain accuracy requirements for subsequent gravity modelling.

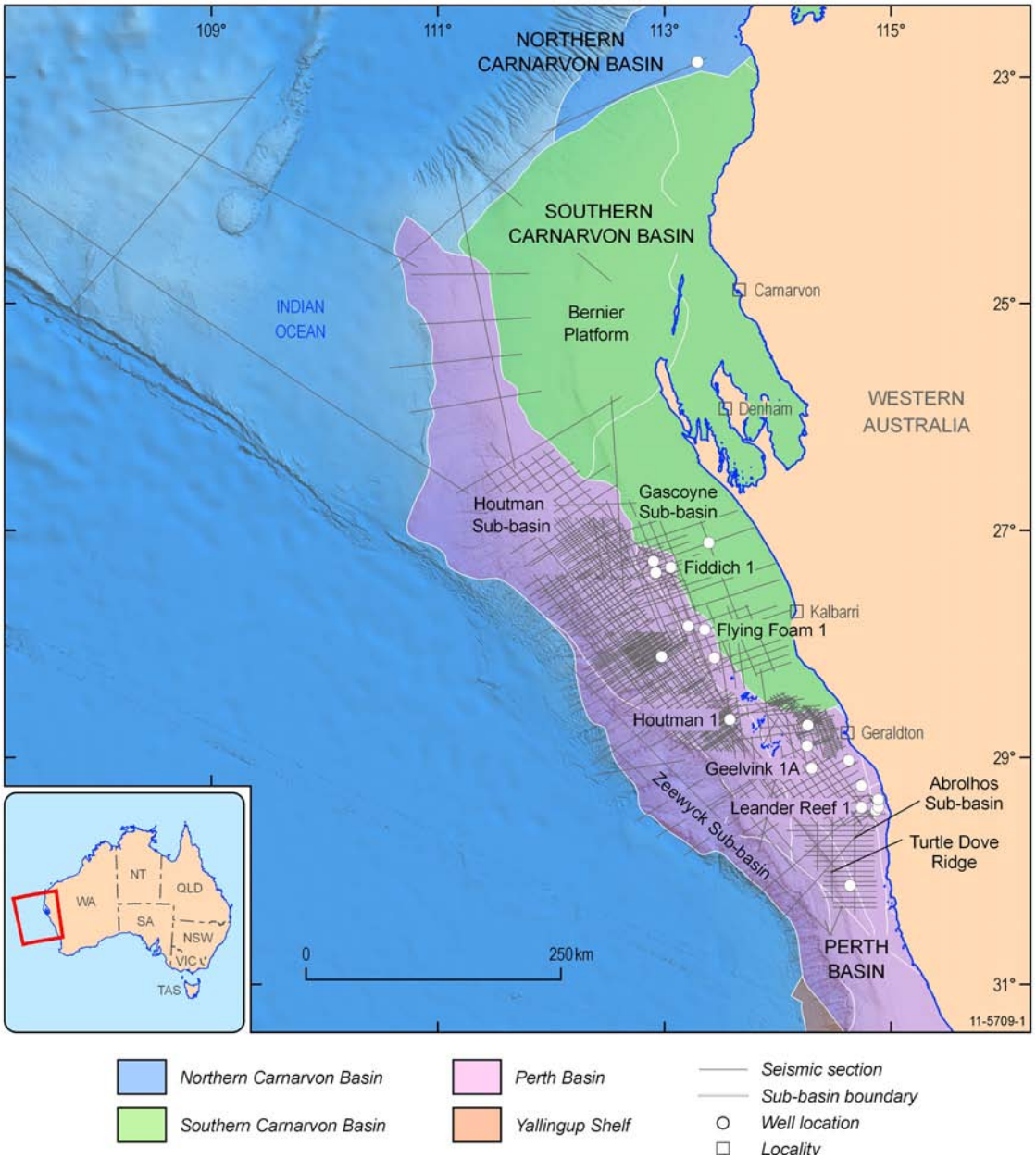

Figure 1: *Distribution of the 541 seismic lines (black) and 19 wells (white circles) used in this study. Sub-basins of the Perth Basin are labelled.*

Estimation of required accuracy

The required accuracy of depth conversion must be linked to a specific task for which the depth conversion is needed. The reason for this particular depth conversion of seismic interpretation in the northern Perth Basin is to provide constraints for gravity modelling. One source of error in gravity modelling is the mis-positioning of the sediment-basement interface due to erroneous depth conversion. This is because this interface is a rather large density contrast. The sea floor and the Mohorovičić discontinuity (Moho) are two other interfaces that are associated with large density contrasts and make major contributions to a gravity model response. The sea floor in our study area is very well constrained and thus gravity anomaly errors associated with its mis-positioning are

negligible. The Moho is not interpreted consistently or confidently in the reflection seismic data, and although mis-positioning of this interface due to erroneous depth conversion can lead to large errors in gravity model response, at present we do not have a reliable base model to test its sensitivity to errors in Moho depth conversion. Therefore, we limit our estimate of gravity modelling accuracy to that resulting from possible mis-positioning of the sediment-basement interface.

To test this, a simple two layer (sediment and basement) scenario was modelled (Figure 2) using the Bouguer gravity equation:

$g_z = 2 * \pi * G * \Delta\rho * t$

Where g_z is vertical gravity, $\Delta\rho$ is the density contrast and t is thickness of sediment overlying basement.

The density contrast was set at 0.47 g/cm^3 to correspond to an expected density contrast between a basement rock (2.77 g/cm^3) and a sedimentary section (2.30 g/cm^3). Three depths to basement were tested that characterise the full possible range of its depth variation: 500, 3300 and 6150 m, with uncertainties of depth respectively ±100, ±500 and ±1150 m.

A ±20 gu uncertainty required for sensible gravity modelling was found to result from a ±100m uncertainty in depth conversion across this range of basement depth variation (Figure 2). The depth conversion method described below was developed to ensure that that depth conversion errors were kept within these bounds.

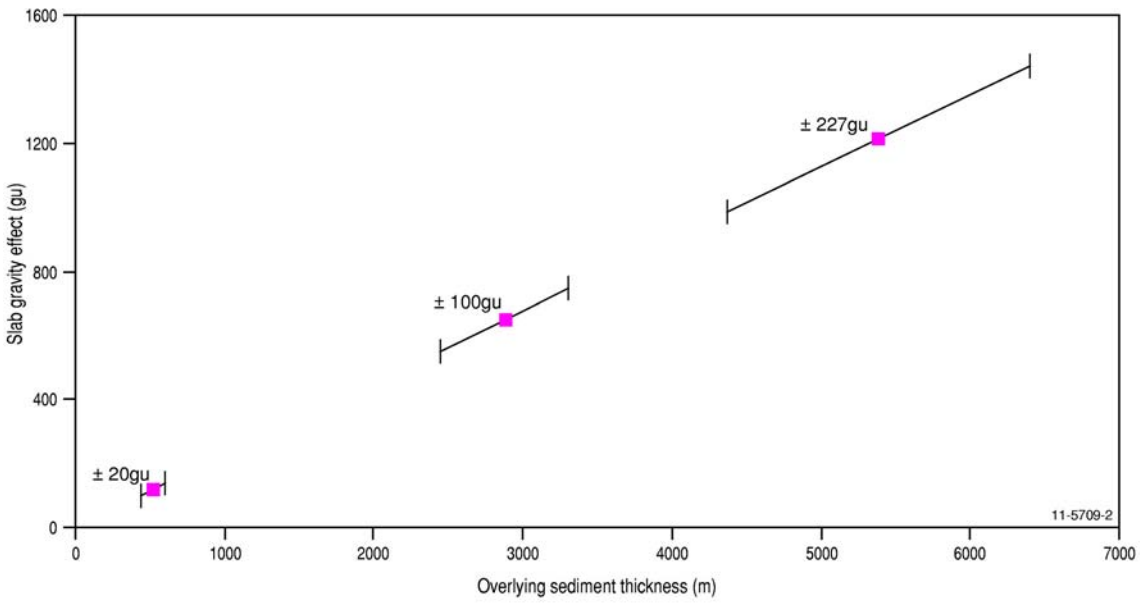

Figure 2: *Slab gravity effect as a function of basement depth and uncertainty in its depth conversion. Assumed density contrast of 0.47 g/cm3 and basement depth of 500±100m (left), 3300±500m (centre) and 6150±1150m (right); the error bars show ranges of gravity variation in response to uncertainty of depth conversion.*

Velocity data

The seismic lines and wells with available velocity data used in this study are shown in Figure 1. Note that there is a far wider distribution of seismic reflection data (and thus stacking velocities) compared to the distribution of wells with velocity measurements.

Stacking velocities are determined from the response of post-stack amplitude of seismic signal to variation in normal moveout (NMO). NMO, in turn, depends on velocity values that are scanned within certain limits in the processing of seismic reflection data. Stacking velocities approach root mean squared (RMS) velocities when the source-receiver offset approaches zero and layers are horizontal and isotropic. The RMS velocity is similar to the average velocity in that it represents the velocity of an acoustic wave through various layers of different interval velocity, though it is usually higher.

A sonic log is a wireline tool run down a well borehole that measures the capacity of a formation to transmit acoustic waves (Rider, 1986). Geologically this is determined by the formation lithology and pore pressure.

A check shot survey is essentially a set of measurements of seismic wave travel times down a borehole. Generally shots are set off in the overlying water column, with geophones lowered incrementally down the borehole.

PRE-PROCESSING OF DATA

All velocity, depth and time information, i.e. the stacking, sonic and check-shot velocities, were compiled (and calculated where applicable) together into an Excel spreadsheet, with one worksheet per well location. Prior to analysis of the data some pre-processing was undertaken, including:

- Error checking and smoothing where applicable (e.g. high-resolution sonic log)
- Reduction of datum to sea floor
- Converting velocity datasets to the same domain (two-way time (TWT) and depth)
- Resampling of datasets to a common TWT interval

The stacking and well velocity datums were shifted to the sea floor to remove the water column from the calculations and also to permit TWT-depth profiles from different locations to be compared.

The conversion of the three velocity datasets to the same domain was undertaken as each dataset is delivered in a different combination of time, velocity and depth. Check shot data are presented originally as functions of TWT versus depth; sonic logs as functions of interval velocity versus depth, and stacking velocities as functions of stacking velocity versus TWT. The calculations carried out to present all types of data uniformly as functions of TWT versus depth are described below.

Stacking and borehole velocities in their original form are sampled at different rates, with time-velocity and time-depth data points not being co-located along vertical profiles. Each of these two data sets had to be resampled to coinciding TWTs in both data sets. This was done by fitting a spline (Akima, 1970) between each TWT-depth data point with a resampled data spacing of 10m. Stacking velocity data below the maximum depth of boreholes were ignored for this process.

Sonic log

Sonic logs were exported from GeoFrame® where they had already been processed for acquisition artefacts and calibrated with available check shot data. Sonic log data contains velocities measured with depth. All sonic logs have been previously calibrated to check shot data.

Most sonic logs had samples taken every 10 cm, leading to a very high resolution 1D log of velocity. As the required depth conversion uncertainty is less than ±100m, the data was smoothed using a 500 point running average and then decimated (every 10th point kept). Velocities were converted to km/s and the reference datums were reduced to the ocean floor.

Sonic log velocities are given relative to log depth, and so needed to be converted to depth versus time. This conversion of sonic log to time was done via the integration method, summarised below:

$TWT_{i+1} = 2*(Z_{i+1}-Z_i)/V + TWT_i$

Where Z is depth (m), V is velocity (m/s) and TWT is two way time (s). The subscript 'i' represents a discrete velocity sample and corresponding TWT and depth position.

Checkshot

All checkshot data were exported from GeoFrame®, and all depth datums were reduced to the sea floor. Velocities were calculated from the time and depth checkshot data by the following formula:

$V_{i+1} = (Z_{i+1} - Z_i) / (TWT_{i+1} - TWT_i)$

Where V is velocity (m/s), Z is depth (m) and TWT is two way time (s). A five point running average was then applied to all velocity data.

Stacking velocity

Stacking velocities were assessed for quality prior to their use in the depth conversion process. The stacking velocity picks from the semblance plots were assessed. For many surveys, the width of high semblance zones within the target TWT intervals was narrow and thus accuracy of corresponding velocity picks was good. For some surveys, common midpoint (CMP) stacks did have ambiguous velocity solutions and corresponding seismic lines were excluded from the calibration and depth conversion process.

Stacking velocity files were received from the Geoscience Australia Data Repository (http://www.ga.gov.au/oracle/npd/) in a variety of different formats. The Western Geophysical format was deemed to be the accepted industry standard and so data were reformatted where necessary. This format is also similar to the VELF format, which additionally contains the spatial coordinates of shot point (SP) locations. All velocity data were then merged into one stacking velocity file for ease of import into the Petrosys® processing package.

A number of surveys presented stacking velocities at CMP rather than shotpoints. To create a uniform dataset, these had to be converted to SP. As the relationship between CMP and SP is linear, the strategy for conversion was to identify the CMP and SP value at three points along a seismic line and then construct a linear relationship between the two.

Stacking velocities for a number of seismic lines were given in reverse order. The error was identified as the trend of the water bottom velocities was opposite to that of the water bottom seismic horizon.

The ocean floor pick in the seismic stacking velocities often occurred below that picked by the seismic interpreters. This gap results in a 'zero' velocity, causing any depth conversion to give a spurious result. To fix this problem, a water velocity ($1500ms^{-1}$) was added at zero seconds TWT where needed.

As with the sonic logs and check shot surveys, stacking velocities were expressed as function of depth below sea floor. The first non-water velocity (i.e. that exceeding 1500 m/s) reported in the velocity file was assumed to characterise the interval from the sea floor to the first pick below it. The

pick immediately above it was assumed to correspond to the seafloor and its calculated depth was set to zero. The formula for converting stacking-derived time-velocity information to depth is given below:

$$Z_i = TWT_i * V_i/2/1000 + Z_{i-1}$$

Where Z is depth (m), TWT is two way time (s) and V is stacking velocity (m/s).

Analytic time-depth function

A one dimensional (1D) analytic time-depth function is often used for depth conversion of seismic interpretation (e.g. Petkovic, 2004) due to it being easily implemented and producing good results for regional studies with fairly homogenous geology. However, the velocity field of the northern Perth Basin is sufficiently heterogeneous to reduce the accuracy with which a 1D depth conversion function could be utilised for the whole basin (e.g. Figure 3). However, to assess possible errors, an analytic velocity function for the northern Perth Basin was developed and depth conversion resulting from its implementation was compared with the depth conversion based on the calibrated stacking velocity method described below.

Two time-depth functions were created using the least squared method with the sea floor as a common datum. The first function was created using the entire velocity dataset and the second using only the upper 10 km of velocity data. A second-order polynomial was constructed to describe a generalised relationship between TWT and depth, with the equation presented in Figure 3 and Figure 4. These figures show that when applying a function for a given TWT, there is a large error in the resulting depth. For example, the depth equivalent of 1 s TWT is approximately 2 km from the formula created using the entire velocity dataset, but it may vary from 1 to more than 3 km in different parts of the basin depending on a specific velocity function (Figure 4). This large discrepancy is due to the variable velocity structure of the basin.

The difference between the two time-depth functions is most apparent in the upper 5 km depth range (Figure 4). The function fit using the upper 10 km of velocity data fits more closely to the well velocities than does the function that encapsulates the entire velocity dataset, which suggests that it describes the subsurface velocities of the offshore northern Perth Basin more accurately. The outcome of this difference between the two functions is highlighted below in Figures 12 to 14.

Due to the large discrepancies in depths when using the time-depth function, depth conversion of 2D seismic interpretation in the northern Perth Basin was undertaken using stacking velocities and the calibration method described in the next section. A visual comparison between depth conversion using the analytic time-depth function and stacking velocities is given below (Figure 15).

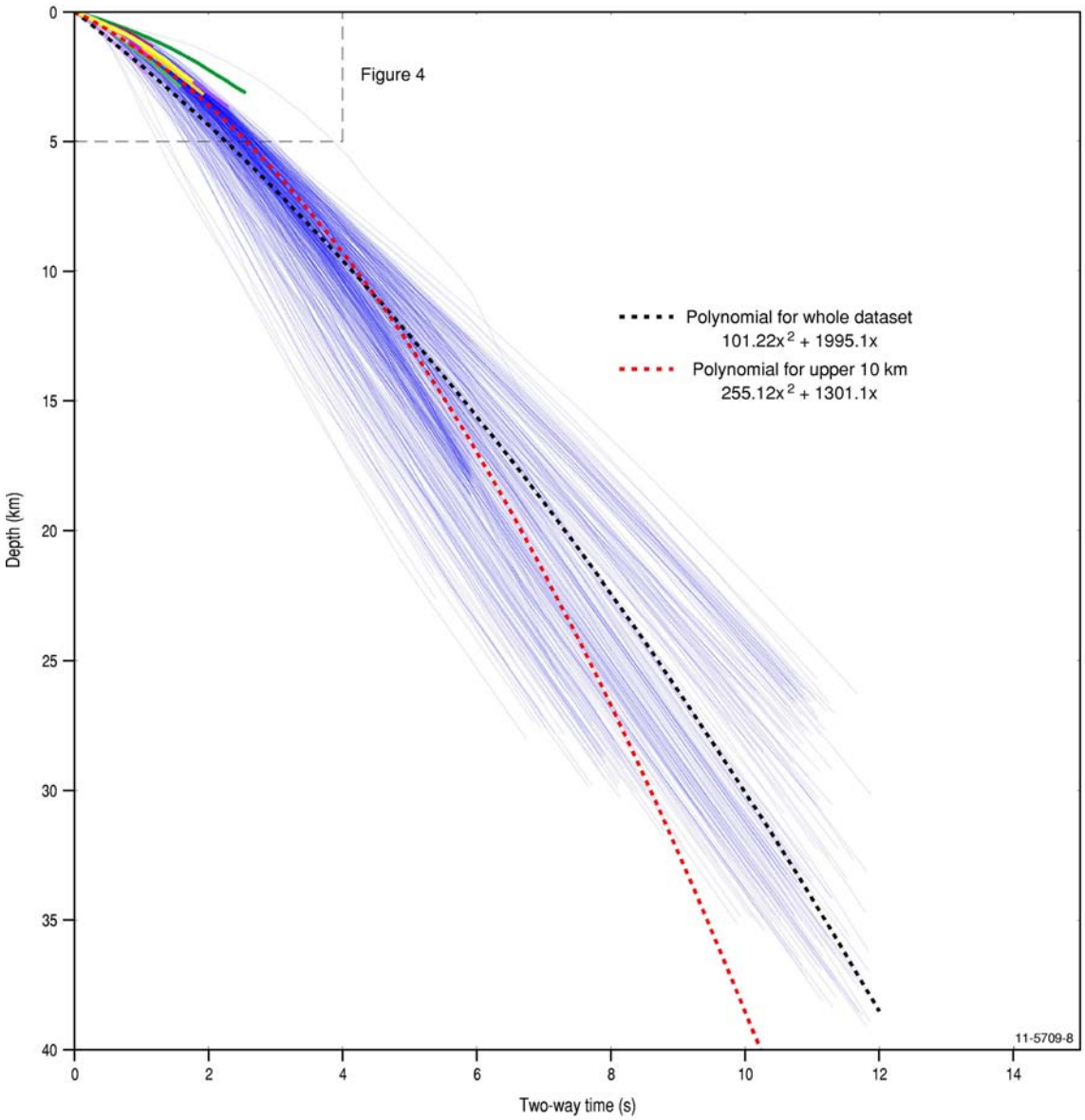

Figure 3: *Compilation of all stacking velocities (blue curves) and well velocities (coloured curves) within the northern Perth Basin and a second order polynomial function fit by least squares method. Note that the depths have been reduced to a sea floor datum.*

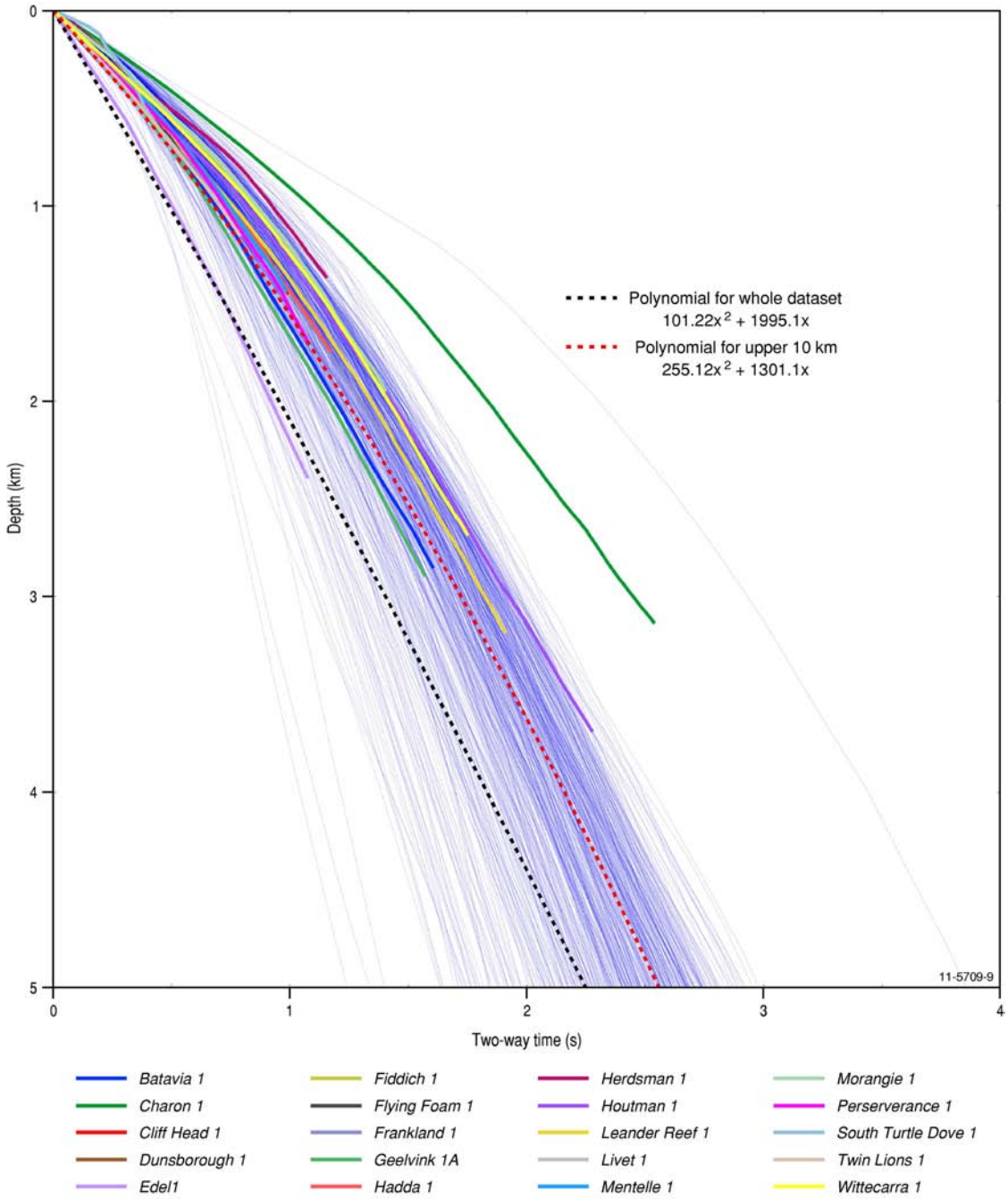

Figure 4: *A close up of Figure 8 showing the relationship between well and stacking velocities. Note the large range of depths that could be calculated at a certain TWT; the velocity structure of the basin is too variable for a single TWT to depth function to be successfully applied. The black dashed line is the analytic time-depth function for the entire velocity dataset, the red dashed line is the analytic time-depth function for the upper 10 km of the velocity dataset.*

Calibration of borehole and stacking velocities

Borehole and stacking velocities were analysed to calculate calibration coefficients that can be used to correct stacking velocities. Sonic logs were used preferentially during the calibration process because of the higher resolution obtained by the tool relative to a check shot survey. Because sonic logs were previously calibrated to check shot, the time-depth relationship between these datasets is essentially the same (though this depends on the quality of the calibration). Check shot data were used where sonic logs were not available or had not yet been calibrated.

The following workflow describes the calibration process:

1. Check each velocity dataset for errors
2. Modify the datum of each dataset to the sea floor
3. Convert all datasets to TWT and depth domain
4. Resample all velocity datasets to the same depth intervals
5. Cross plot stacking velocity depths near a well site with corresponding well depths
6. Fit a linear polynomial to this cross-plot (higher order polynomials were tried also), and determine calibration coefficient from the gradient of the polynomial.
7. Grid calibration coefficients
8. Multiply depths derived from stacking velocities by calibration coefficient grid

The velocity datasets were compiled into an Excel spreadsheet. A worksheet was added for each well in the northern Perth Basin, with appropriate sonic log, check shot and stacking velocity profiles. Graphs were created of TWT versus depth from the borehole logs and from several stacking velocity profiles adjacent to the well. These graphs show how the stacking velocities change away from the borehole, as well as the difference between coincident well and stacking velocity profiles (red line of Figure 5).

Depths calculated using stacking velocity profiles (SD) at locations adjacent to a well were presented as functions of well depth (WD) from the well measurements (Figure 6). This is achieved through taking readings of both SD and WD at a set of fixed two-way times (made possible through the resampling of each dataset). The resultant SD-WD cross-plots enabled calculation of the required calibration coefficients (Figure 6), as described below.

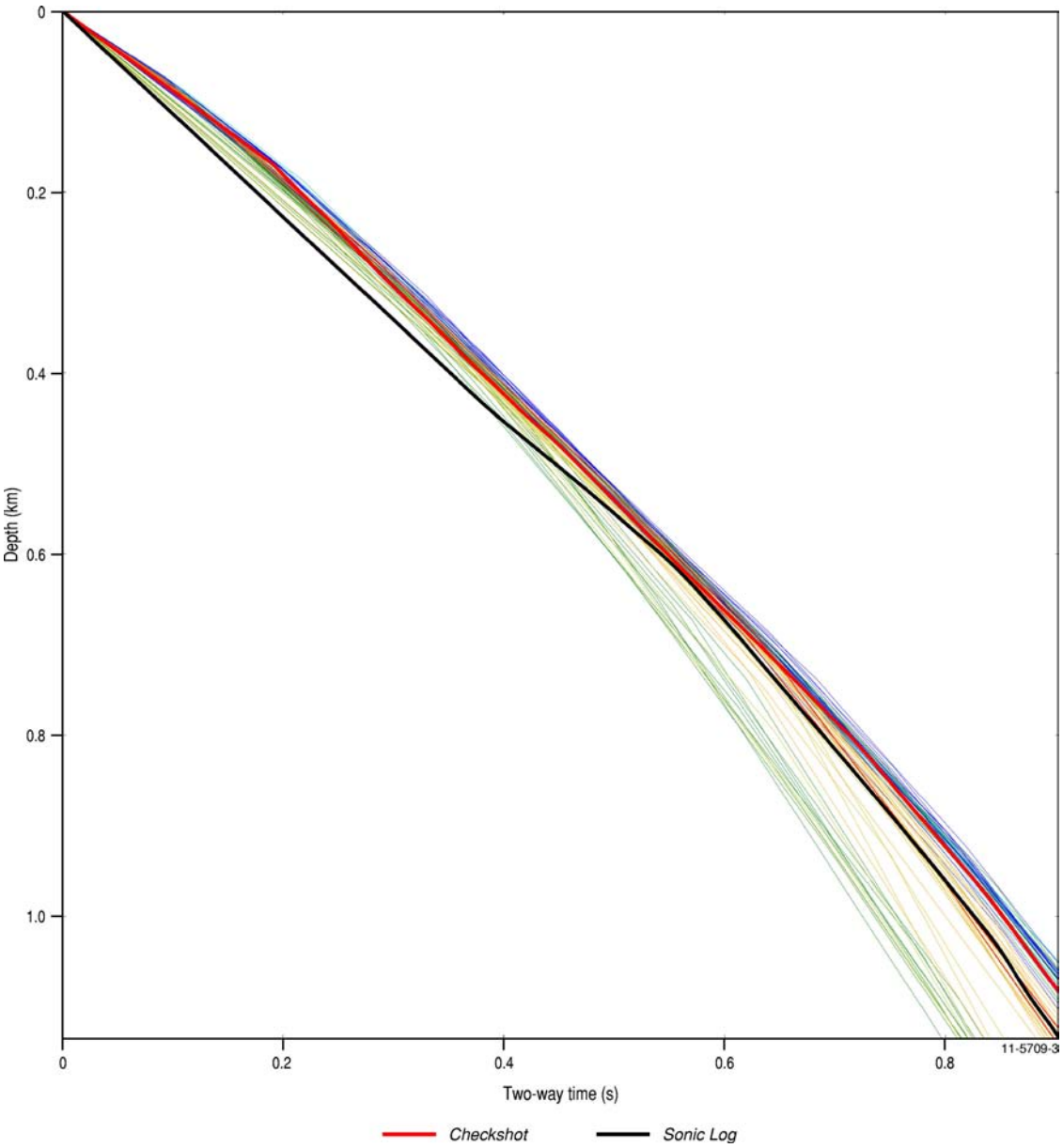

Figure 5: *Two-way time–depth (TD) functions from sonic log and check shot measurements in Fiddich 1 well (black curve) compared to TD functions from stacking velocity analyses adjacent to well location. Red – from stacking velocity analyses closest to well location, orange – within 100SP, yellow 100-200SP, green 200-400SP, cyan 400-600SP, blue more than 600SP from the well location.*

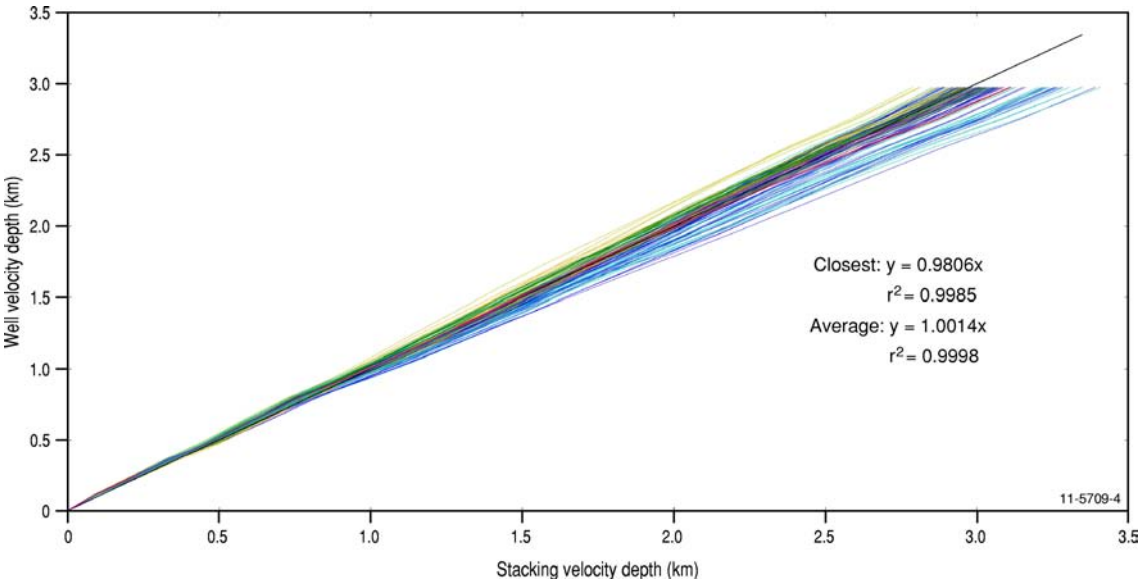

Figure 6: *Cross-plot of depths calculated using stacking derived velocities (SD) at several locations adjacent to well versus well depth (WD) for Leander Reef 1 well and stacking velocity from seismic line S89-101ARl. The colour code is the same as in Figure 5. Solid black line is a 'no distortion line': where the SD and WD are the same, they plot on this line.*

CALCULATION OF CALIBRATION COEFFICIENT

Stacking velocities were calibrated against well velocities to minimise their differences, resulting in better depth conversion of seismic interpretation from seismic stacking velocities. We used the TWT-depth functions (e.g. Figure 4) for calibration purposes rather than velocity-depth, or velocity-TWT functions. This is because the relationship of velocity with depth or TWT is not as simple as depth versus TWT and a more complicated calibration method would be required.

Using the regularised resampled datasets, cross plots of stacking velocity profile depth versus well velocity depth were created (e.g. Figure 6 and 7). These plots are used to visually and numerically show differences in stacking and well depths: if depths are equal, they will plot along a line with gradient of one; if they differ, they will deviate from this line. Stacking velocity depth calibration coefficients were derived by fitting a polynomial to the SD-WD curves, with the gradient of this polynomial being the calibration coefficient. The calibration coefficient is applied by multiplying it by depths calculated using stacking velocities. This multiplication can be visualised as rotation (clockwise or counter-clockwise depending on the specific SD-WD relationship) of the SD-WD linear trend to become co-aligned with the no distortion line in the SD-WD cross-plot (Figure 6). The multiplication of the SD-WD linear trend by this coefficient has the effect of calibrating SD against WD to make the stacking derived depths (e.g. seismic interpretation depth converted using stacking velocities) better match the depths at the well site. We calibrate already calculated depths, rather than TWT interpretation, because the calibration coefficient was calculated on depths rather than TWT. Table 1 shows the calculated calibration coefficients for the offshore northern Perth Basin.

For testing purposes, second- and third-order polynomials were also fit, though their solutions are not as stable as the linear ones (especially near the bottom of the borehole) and calibration coefficient maps resulting from non-linear approximations are more difficult to implement, as the coefficient varies with depth. While many stacking velocity profiles near the well were plotted on the graph, only the closest profile was used to create the calibration coefficient. This is because the geology varies away from the well site and only the semblance plot for this stacking velocity profile was examined to ensure that the velocities derived from it were of good quality.

Graphs of the difference between well depth and calibrated stacking depth were created to show differences in calibrated depths with depth down the well (e.g. Figure 7). These graphs show that as one calibrates stacking velocity profiles away from the well, the error generally increases. This is due to the spatial variability of the northern Perth Basin geology.

Table 1: *Calculated calibration coefficients for wells in the offshore northern Perth Basin. Figure 8 and 9 show grids of these values.*

Well	Calibration coefficient
Charon 1	0.72
Twin Lions 1	0.95
Livet 1	0.95
Herdsman 1	0.95
Wittecarra 1	0.97
Leander Reef 1	0.98
Morangie 1	0.98
Frankland 1	0.99
Cliff Head 1	0.99
Mentelle 1	1.00
Perserverance 1	1.02
Dunsborough 1	1.02
Fiddich 1	1.02
Houtman 1	1.03
Batavia 1	1.03
Geelvink 1A	1.04
Hadda 1	1.11
Flying Foam 1	1.21
Edel 1	1.47
South Turtle Dove 1	1.52

A Python script was written that implemented the above workflow. The script handled reading data from each worksheet in the Excel spreadsheet, resampling the datasets to a common TWT interval and calculating and plotting the calibration coefficient, as well as various accuracy metrics.

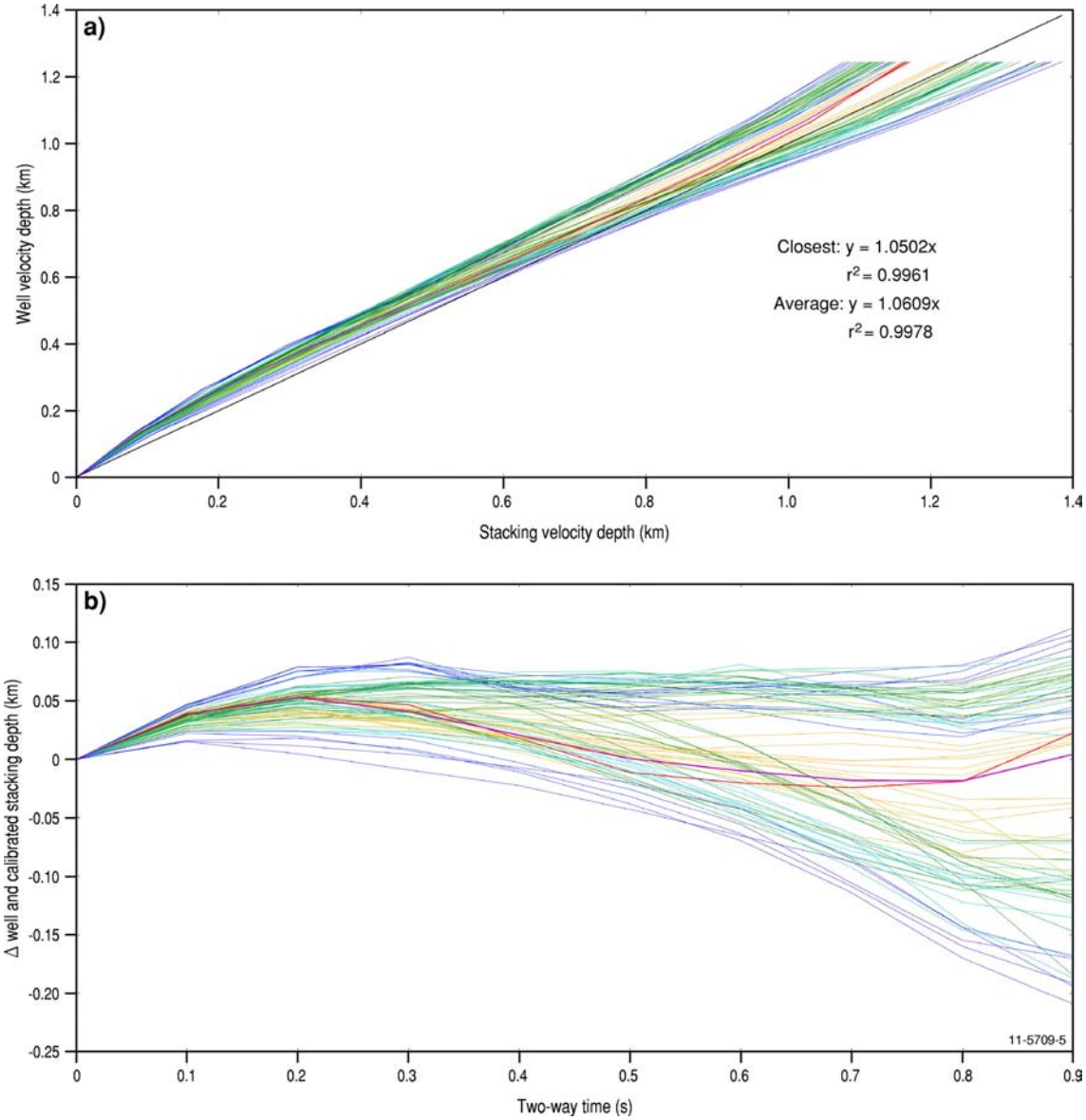

Figure 7: *(a) Cross-plot of depths calculated using stacking derived velocities (SD) at several locations adjacent to well versus well depth (WD) for Flying Foam 1 well and stacking velocity profile from seismic line E92AU08-25R. Solid black line in (a) is a no distortion line: in the case of a perfect SD-WD calibration the SD and WD would be the same and plot on this line. Line colour is the same as in Figure 3.; (b) Difference between WD and calibrated SD as a function of TWT. Note that maximum difference between WD and calibrated SD at closest location does not exceed 50 m down to well bottom (red line in (b). Maximum difference between WD and calibrated SD from an average of 200m either side of the closest location is shown in purple.*

APPLICATION OF CALIBRATION COEFFICIENT

Using the above methodology, we have calculated a calibration coefficient for each well-seismic intersection. It must be discussed how these coefficients are interpolated throughout the offshore northern Perth Basin to other seismic surveys, or indeed whether interpolation is a suitable strategy.

Several methods for extrapolating the calibration coefficients away from wells were investigated. The first was to simply grid the calibration coefficients using a minimum curvature algorithm (Figure 8). The second method was to force the calibration coefficient grid to tend to one away from the wells (Figure 9). This has the effect of simply preserving depths calculated using stacking

derived velocities away from wells. The reason for this approach was that it is unknown how stacking and well velocities correlate away from well sites.

Depths to interpreted horizons are calibrated by multiplying the interpolated calibration coefficient at each location with a depth calculated by a stacking-derived velocity. This can be done using an average or interval velocity calculation from stacking velocities either on a line-by-line basis, or for a grid.

A comparison between the two approaches taken to extrapolate calibration coefficients is given in Figure 10. This figure shows the Valanginian Unconformity horizon depth converted and then calibrated using both the unconstrained and the forced calibration coefficient grids; the difference between these two calibrated grids is also given. Figure 10c shows that there are indeed significant differences in the resulting calibrated depth horizon that stem entirely from the methodology used to grid the calibration points. The differences are generally smaller in the near vicinity of wells but increase with distance away; this will be caused by the unconstrained version of the calibration coefficient grid. Because the work that uses results of this depth conversion methodology is focussed around wells e.g. the burial history modelling of Pfahl (2011) and gravity modelling, we chose to use the constrained calibration coefficient grid for depth conversion work. As such, all further examples of calibrated depth conversion within this document use this constrained gridded calibration coefficient grid.

A consideration to take when extrapolating the calibration coefficients away from the well sites (in order to calibrate all seismic stacking velocities in the basin) is the geology that the well intersects and how the rock properties at the well site vary spatially. Are there any significant differences in lithology between sub-basins that may cause abrupt changes in velocity? Perhaps extrapolating the calibration coefficients away from the well is not tenable? Geologically constrained calibration coefficient grids have not yet been generated. This would involve examining how calibration coefficients are interpolated between sub-basins and around structural features, such as basement highs.

The calibration coefficient is a qualitative indication of how well stacking velocities compare to direct measurements of seismic velocity from boreholes and cannot be used to infer anything about the geology at the well site. However, the calibration coefficient may be used as a first pass assessment of the quality of seismic stacking velocities, relative to well velocities, where they are employed as a tool used to understand the velocity structure of the sub-surface (e.g. Mjelde et al., 2007; White et al., 2008).

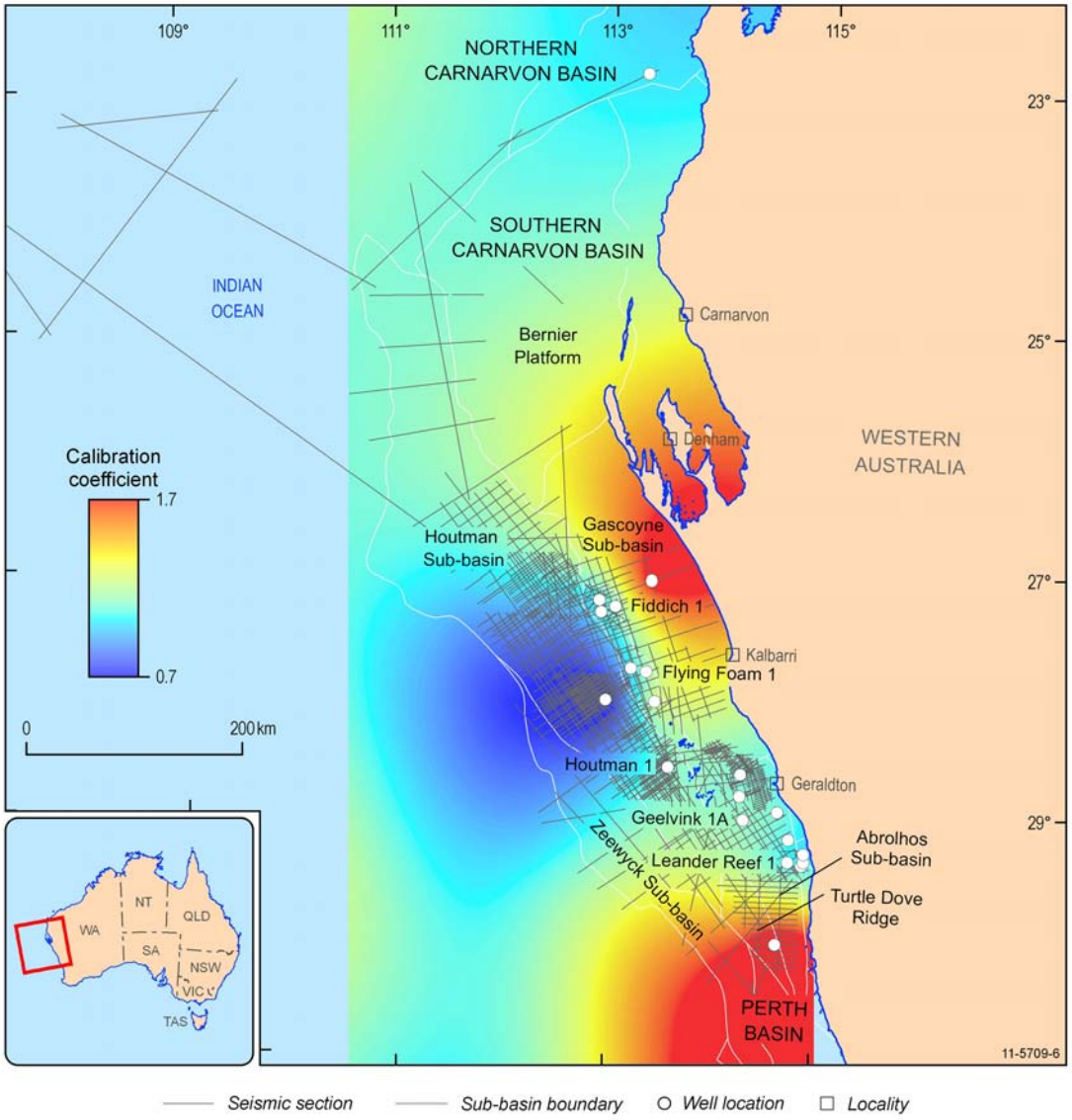

Figure 8: *Calibration coefficient grid created by minimum curvature gridding of calibration coefficients calculated at well sites (white circles).*

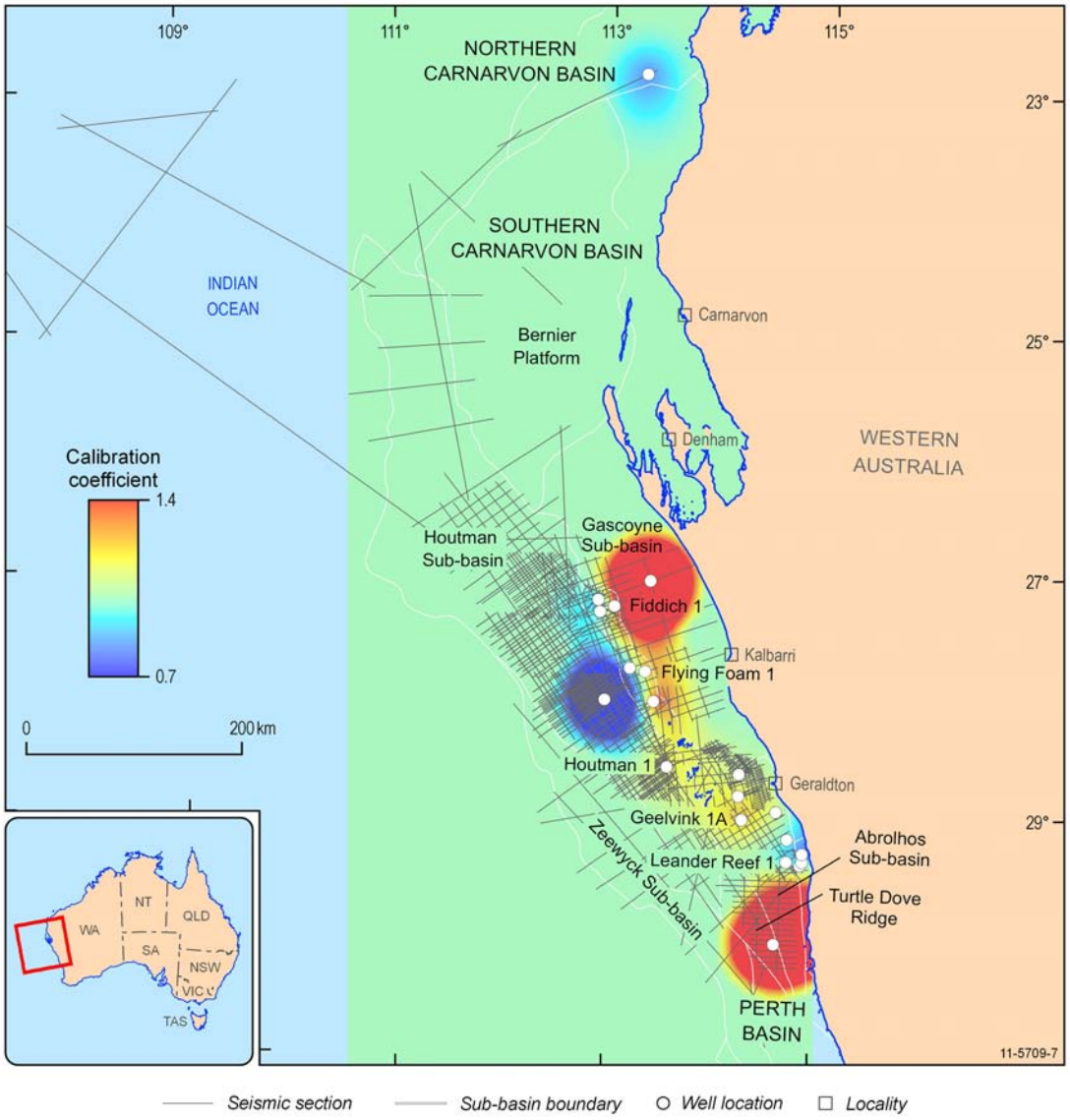

Figure 9: *Calibration coefficient grid created with dummy 'one' values located around the calibration coefficients calculated at well sites (white circles).*

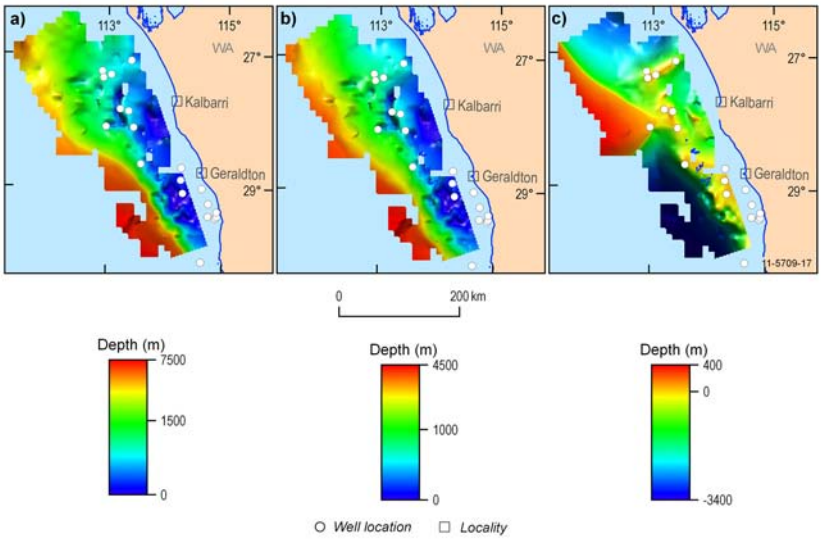

Figure 10: *A comparison of the different methods of gridding calibration coefficient using the Valanginian Unconformity horizon; a) shows the Valanginian Unconformity depth horizon calibrated with unconstrained gridding (Figure 8), b) shows the Valanginian Unconformity depth horizon calibrated with dummy one values (Figure 9) and c) shows the difference between the two grids. There is substantial difference, especially away from the well locations (white circles).*

Depth conversion error estimation

An analysis of the discrepancies between depths calculated from stacking velocities and measured borehole depths was undertaken to ascertain whether the calibrated depth conversion method would provide sufficiently accurate depth conversion.

The error analysis was done in two parts:

1. By assessing the difference between stacking velocity derived depth and well depth at a number of points regularly spaced down the well, and
2. Comparing the stacking velocity derived depths of various seismic sequence boundaries with corresponding well sequence boundaries.

WHOLE OF WELL ERRORS

The difference between stacking velocity derived depth and well depth for all wells in the offshore northern Perth Basin is shown in Figure 11. The graph shows that the difference between stacking velocity depth and well depth varies with depth, but is generally less than 50m and, except for one case, is less than the target for gravity modelling considerations (e.g. ±100m). Average discrepancies are shown in Figure 12, highlighting that the errors are kept to below 50m for the entire well depth. Note that there is no way to identify errors below the maximum depth of the wells and thus there is no way to calibrate the seismic stacking velocities either.

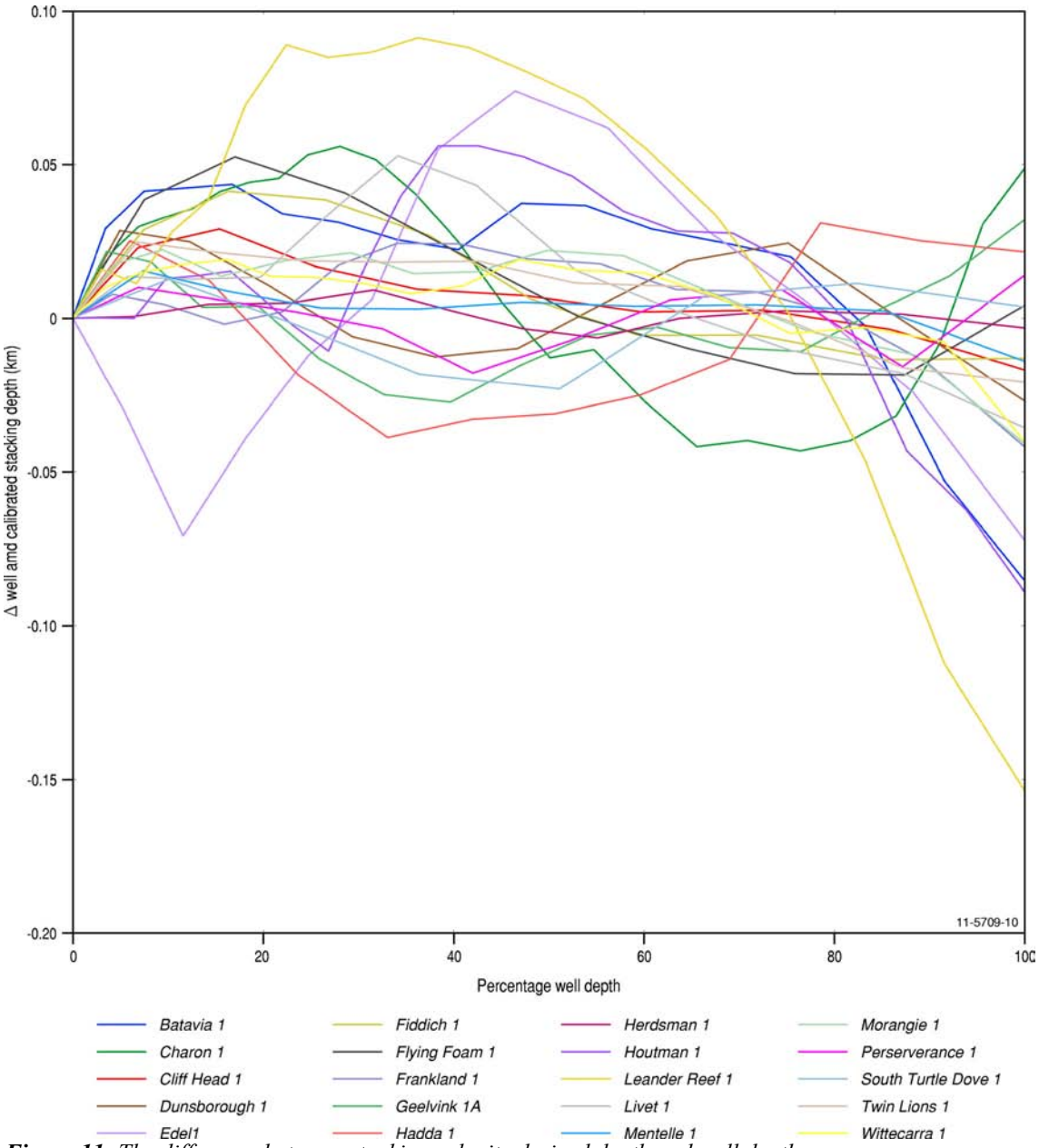

Figure 11: *The difference between stacking velocity derived depth and well depth as a percentage of well depth. Discrepancies were calculated for resampled depth points to achieve regular spacing down wells. For most wells the discrepancy is less than 50m.*

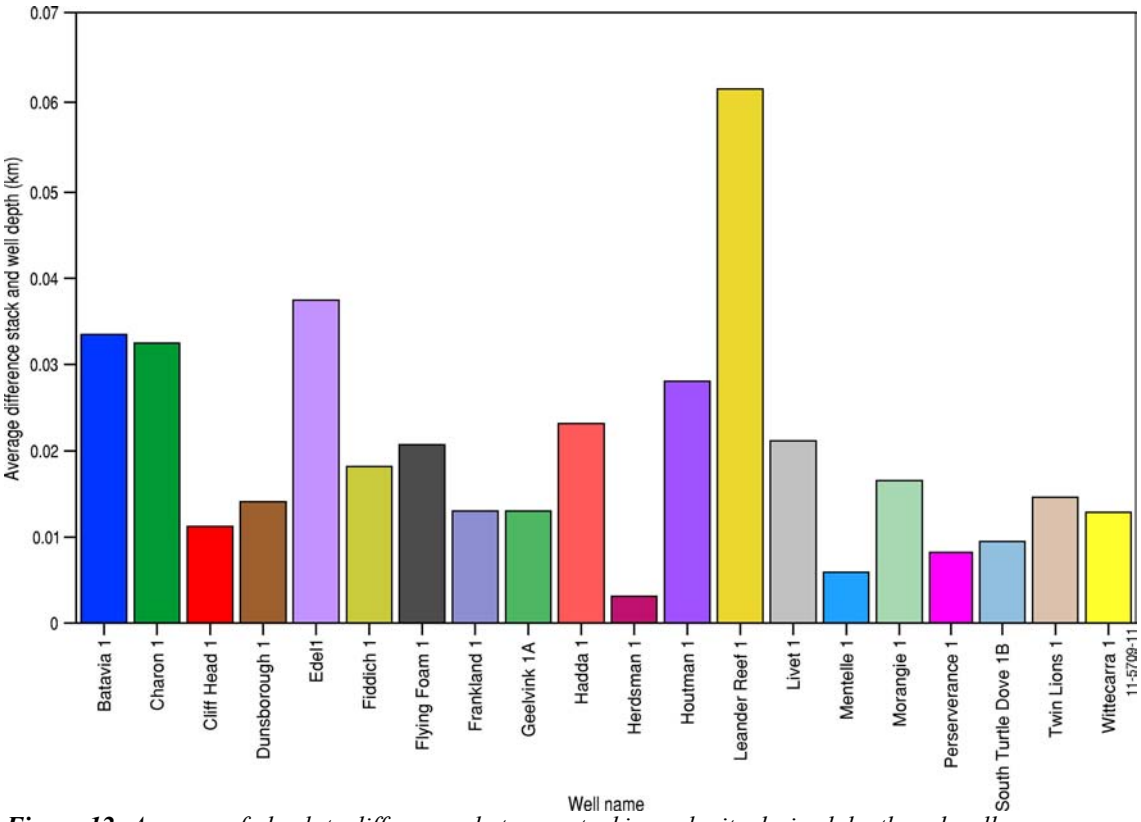

Figure 12: *Average of absolute differences between stacking velocity derived depth and well depth. Generally the average difference is less than 50m.*

GEOLOGICAL HORIZON ERRORS

The depth converted interpreted seismic horizons were compared to corresponding geological horizons identified in well logs and cuttings. Three seismic (and corresponding geological) horizons were chosen for comparison: Valanginian Unconformity, base of Yarragadee and a Late Permian horizon.

Figures 13 to 15 show the normalised difference between depth-converted seismic interpretation and well depth for the three horizons for four different depth calculations:

1. Uncalibrated seismic stacking velocities
2. Calibrated seismic stacking velocities
3. Analytic TWT-depth formula (0 – 10 km depth)
4. Analytic TWT-depth formula (0 – 40 km depth)

The differences are shown in Table 2. The normalised difference is calculated by subtracting the seismic depth from the well depth, dividing it by the well depth, then taking the absolute value. Generally the calibrated seismic stacking velocity derived depth is better than the uncalibrated, and, except for Batavia 1, the seismic stacking velocity methods are always better than the analytic function. For each of the horizons, there seems to be a maximum of 30% difference between depths to seismic horizon and depth to corresponding formation in a well. However, this may be due to the discrepancy between where the seismic horizon and well depth are interpreted rather than due to depth conversion error. Often the seismic interpretation is not exactly at the correct depth and in places the well depth is uncertain due to limited geological information. So, for the time being we believe that the whole of well errors described in the previous section are a better measure of depth conversion accuracy.

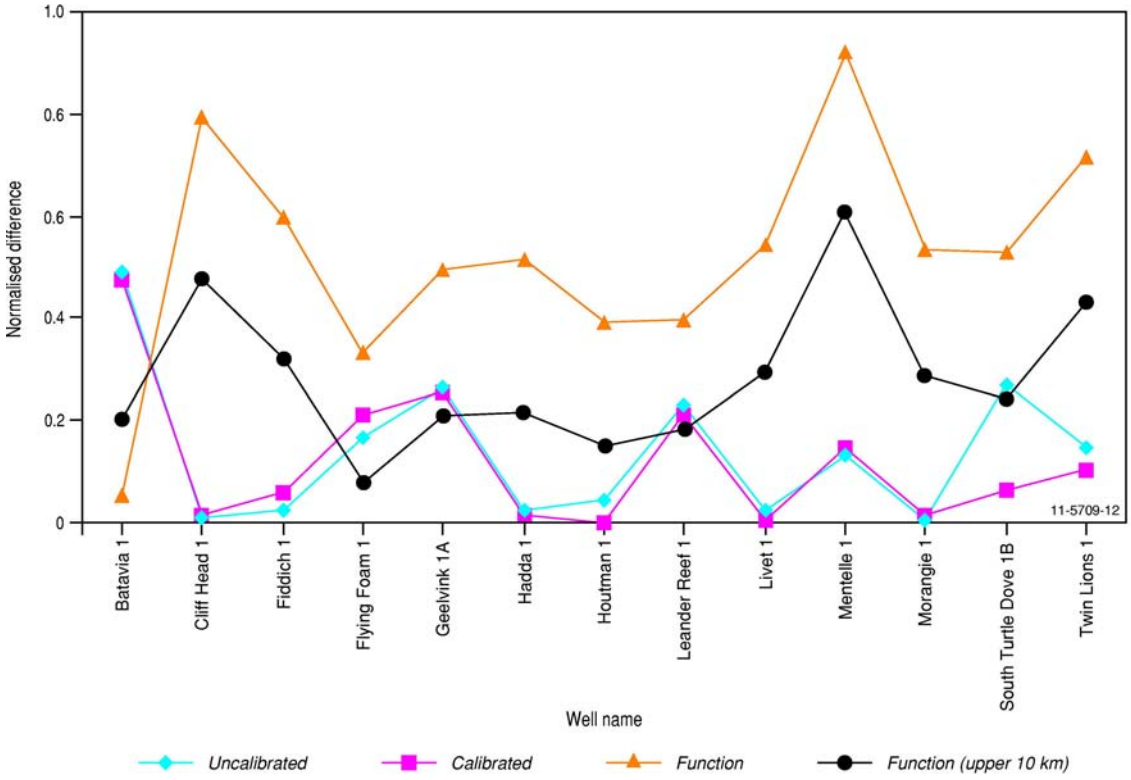

Figure 13: *Normalised difference between depth-converted seismic interpretation of the Valanginian horizon and well depth.*

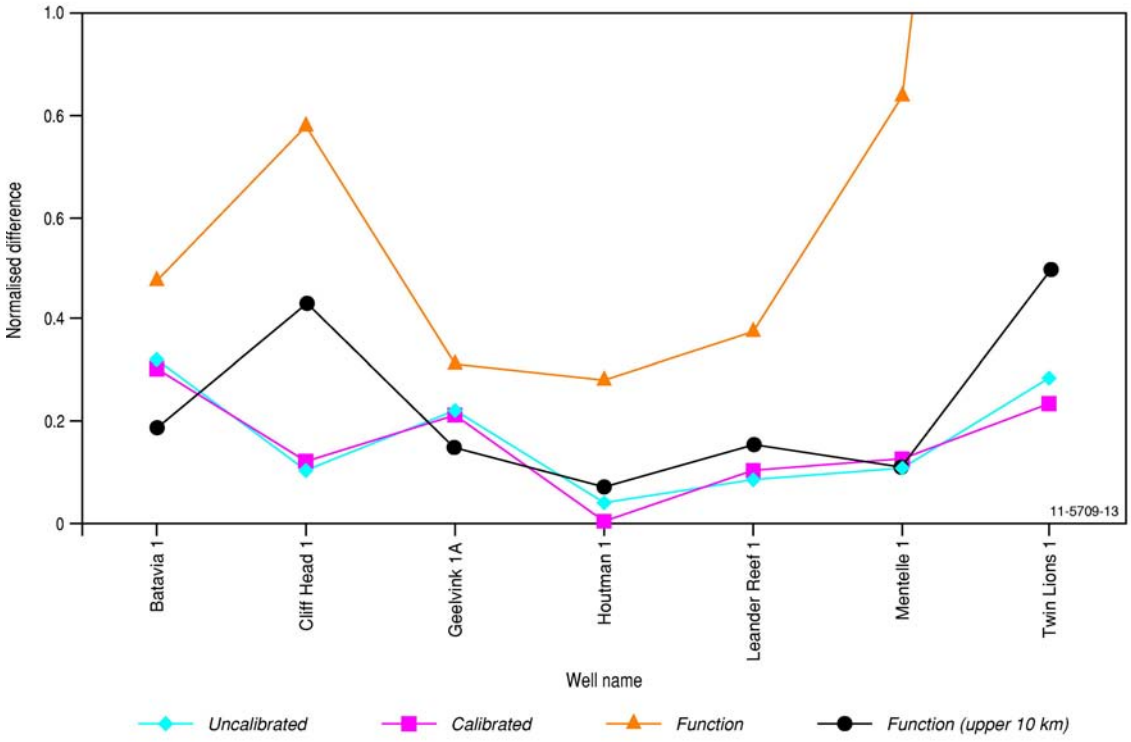

Figure 14: *Normalised difference between depth-converted seismic interpretation of the Yarragadee horizon and well depth.*

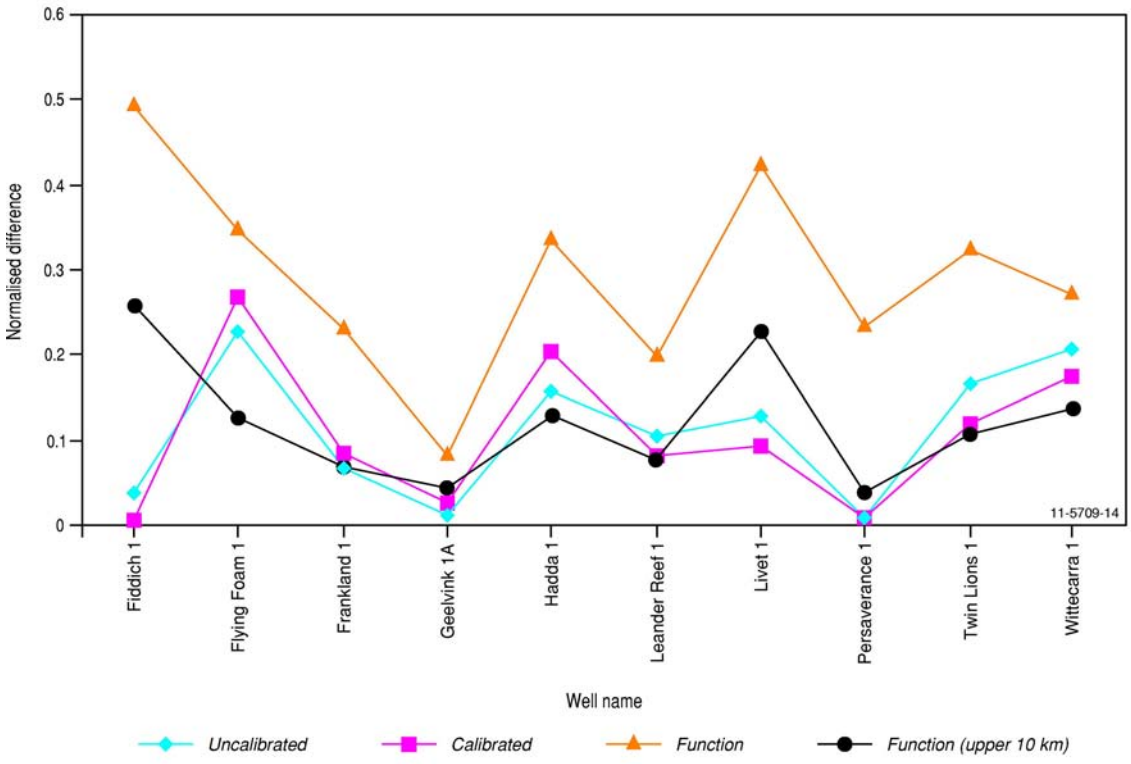

Figure 15: *Normalised difference between depth-converted seismic interpretation of the Late Permian horizon and well depth.*

Table 2 shows a detailed break down of the differences between uncalibrated, calibrated and analytic function derived seismic depths and well picks. From the calculated seismic depth and well interpretation it can be inferred that on average the calibrated stacking velocity depth conversion performs better than the uncalibrated one and better than the analytic function method. It must be noted that differences between the seismic horizon and well pick are present regardless of the preferred depth conversion method and must be taken into account. Estimated errors in depth conversion are within an acceptable range for gravity modelling.

Figure 16 shows the effect of depth converting the Valanginian, Yaragadee and Late Permian seismic horizons interpreted using un-calibrated and calibrated stacking velocities and the two TWT-depth functions, for seismic line E92Au09-41R. This seismic line shows the wide range of depths that can be calculated from the various methods. The un-calibrated and calibrated stacking velocities and function using the upper 10 km show some similarities in the resulting depths, with the function using the entire velocity database being much deeper. Table 1 and Figures 13-15 show that at the well sites, the function created using all available seismic velocities has much larger discrepancies between depth-converted seismic horizons, so it can be inferred that these deep depths on E92Au09-41R are incorrect.

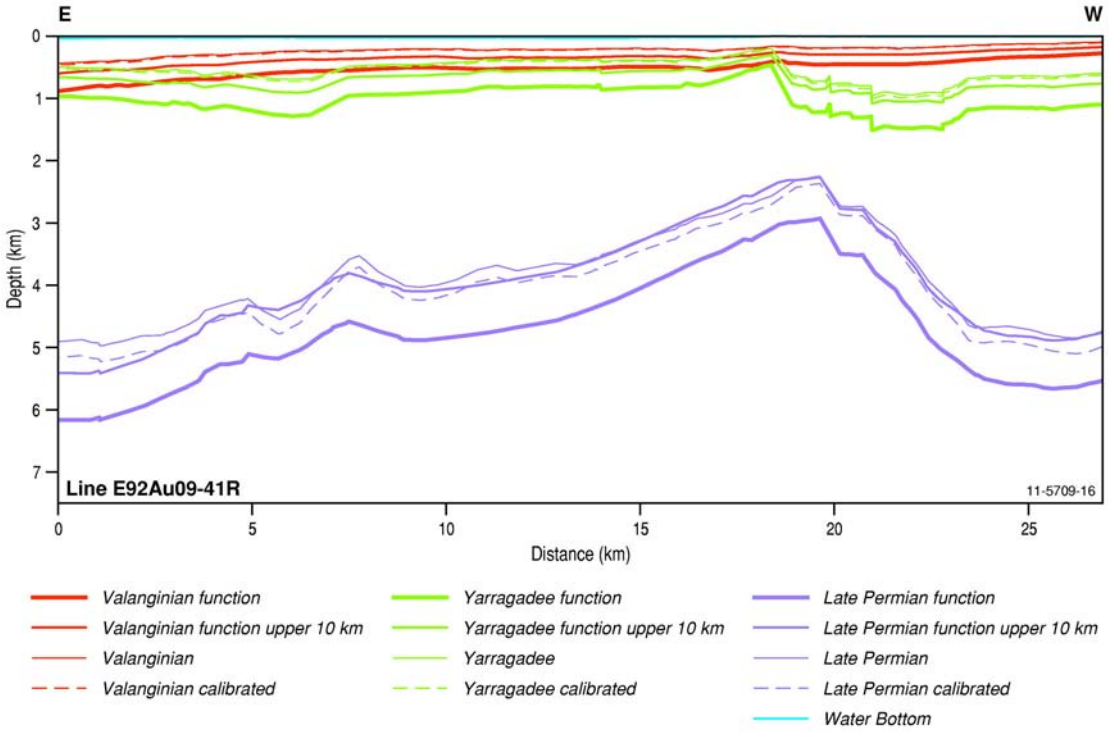

Figure 16: *Valanginian, Yarragadee and Late Permian horizons interpreted on seismic line E92Au09-41R and depth converted using the analytic functions and un-calibrated and calibrated stacking velocities. A wide range of depths are calculated using these four methods. The analytic function that takes into consideration the entire velocity dataset gives results that are the deepest, most different from the other three methods and have the largest discrepancies at well sites (Table 2).*

Table 2: *Difference between un-calibrated, calibrated, analytic function for whole velocity dataset and analytic function for upper 10 km derived seismic depths and well depths for three key geological horizons in the northern Perth Basin. While the calibrated depth did not prove to be the smallest difference on individual wells, overall the average difference is less, with the analytic function showing the largest discrepancy. The analytic function for the upper 10 km has a smaller depth conversion error than the function fit for the entire velocity data set. Differences between the seismic horizon and well pick, regardless of the preferred depth conversion method, are present and must be taken into account.*

Differences between seismic and well depths				
	Uncalibrated	**Calibrated**	**Function**	**Function (10 km)**
Valanginian				
Batavia 1	-126.0	-122.1	-14.3	-52.4
Cliff Head 1	0.8	-1.5	68.2	40.8
Fiddich 1	17.5	39.2	407.5	217.3
Flying Foam 1	-88.7	-110.7	175.1	42.8
Geelvink 1A	-82.9	-80.6	156.1	66.4
Hadda 1	-13.0	7.6	272.6	112.9
Houtman 1	-33.9	1.3	288.3	111.1
Leander Reef 1	22.8	20.5	38.7	17.7
Livet 1	21.1	-5.4	471.6	254.2
Mentelle 1	-10.2	-11.6	72.3	47.7
Morangie 1	4.4	-11.3	489.1	262.4
South Turtle Dove 1B	-130.9	31.1	256.5	115.6
Twin Lions 1	12.2	8.5	58.7	35.5
Average	-31.3	-18.1	210.8	97.8
Yaragadee				
Batavia 1	-172.1	-161.3	252.1	101.1
Cliff Head 1	-12.8	-14.9	94.0	52.3
Geelvink 1A	-200.2	-193.2	283.5	94.1
Houtman 1	-126.7	14.5	829.9	65.0
Leander Reef 1	-67.0	-81.1	287.3	449.1
Mentelle 1	-13.2	-15.3	101.7	84.5
Twin Lions 1	66.9	55.0	121.7	60.0
Average	-75.0	-56.6	281.5	129.4
Late Permian				
Fiddich 1	47.9	6.0	626.7	328.8
Flying Foam 1	-302.6	-353.7	459.5	167.9
Frankland 1	-150.6	-192.5	518.8	153.6
Geelvink 1A	31.6	78.1	248.0	-131.4
Hadda 1	253.7	328.1	536.4	206.9
Leander Reef 1	319.1	251.3	614.6	234.1
Livet 1	219.9	161.7	728.8	390.0
Perseverance 1	16.2	16.2	370.1	59.3
Twin Lions 1	234.6	169.0	455.1	149.8
Wittecarra 1	581.6	487.0	763.2	382.1
Average	125.1	95.1	532.1	194.1

ERRORS RESULTING FROM STACKING VELOCITY PICKS

Because picking stacking velocities is an interpretive task it is reasonable to assume that different values of stacking velocities may have been interpreted for different surveys close to the same wells. Differences in quality or resolution of stacking velocities may also arise between differing vintages of seismic data. Stacking velocity analysis on lines with different orientation relative to strike of structures may potentially return different velocity values if seismic anisotropy is present in the region (e.g. Tsvankin, 2005).

To highlight where inconsistencies or errors may arise in the use of stacking velocities due to these factors, we consider the Geelvink 1A well. The stacking-derived depths for lines S89-102r and E92AU09-41r correlate differently with the Geelvink 1-A well depths, with linear coefficients of 1.0315 and 1.0515 respectively (Figure 17). That is a 2% difference. The lines in question come from different seismic surveys. The difference in stacking velocity profiles and derived depths between these two close locations highlights that by using stacking velocities to depth convert regional time horizons, we are dependent on the subjectivity of the processing geophysicist and several other factors outlined above, and that the velocities we use are only an approximation of the real rock velocities. In this study, where multiple calibration coefficients were calculated, they were averaged and integrated during the gridding process.

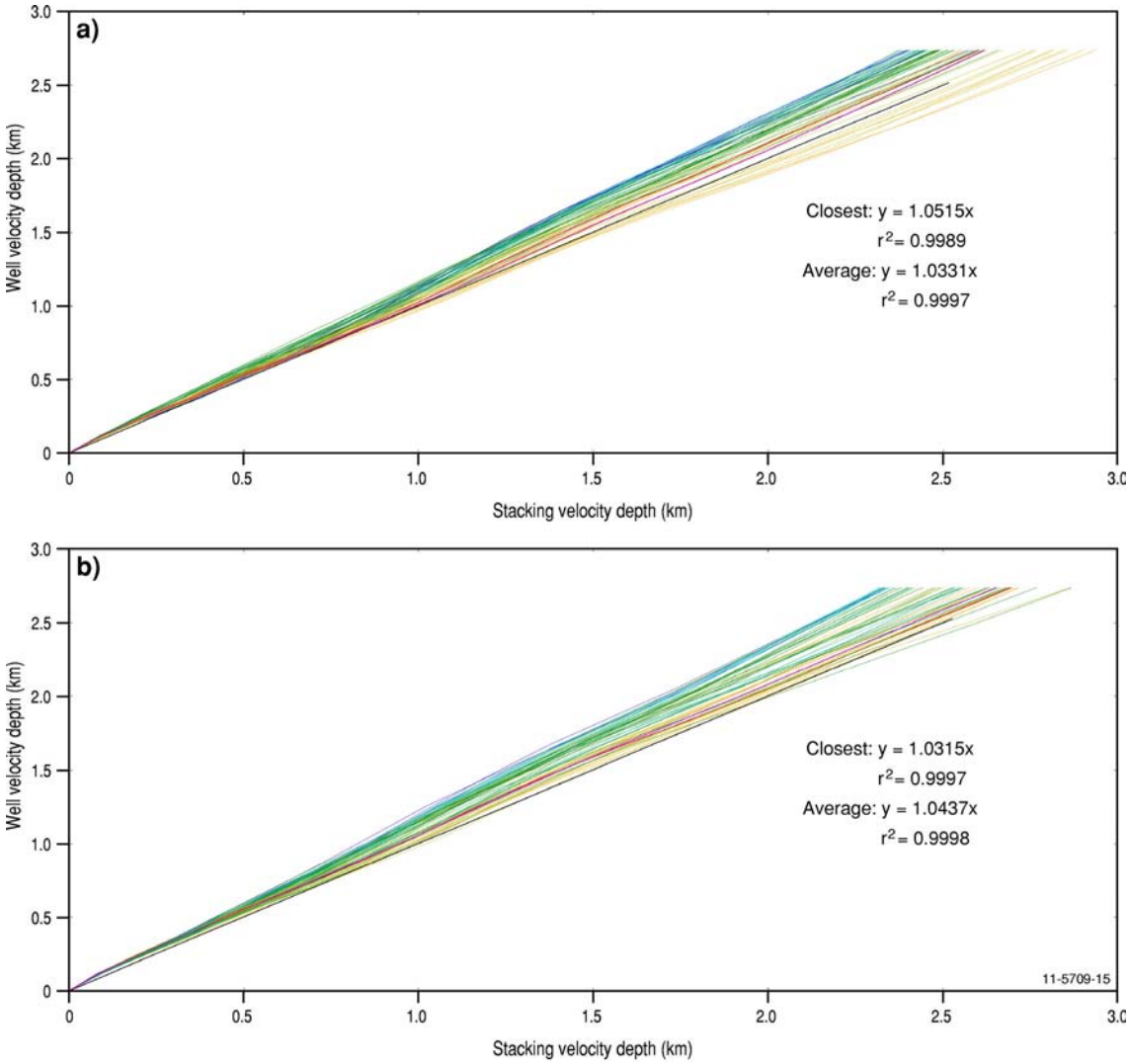

Figure 17: *Comparison of stacking velocity versus well velocity depths for different seismic lines that intersect Geelvink 1A: a) E92AU09-50, b) S89-102.*

Discussion

We have discussed the calculation and application of a stacking to well velocity calibration coefficient to enable more accurate depth conversion for the entire depth of the well. However, in the future it may be beneficial to calculate and apply the calibration coefficient for specific geological intervals, rather than for the entire range intersected by a borehole, e.g. the separate geological units presented in Figure 16. A calibration coefficient calculated at one well may represent a different range of geological units from an adjacent well, based on differences in geology at the well site and in the depths drilled. Defining an interval based upon a geological unit over which well and stacking velocities are compared may decrease overall ambiguities in the calibration coefficient and errors in the resulting depth conversion. Whilst this would require seismic interpretation to be fairly complete throughout the region, in turn it would allow implementation of depth conversion based on interval velocities (Dix, 1955). The induration of geological units with depth may also be considered, as deeply buried strata will have a faster velocity than the same lithology buried to a shallower depth (e.g. Japsen, 1993). Geology and depth-dependant calibration coefficients might thus be further investigated in future work. This would work well in the Abrolhos Sub-Basin of the northern Perth Basin, where geological units are mapped fairly extensively and the thickness of these sequences varies throughout the basin.

As shown above, consideration must be given to how the calibration coefficient is extrapolated away from control points. We examined two scenarios where uncontrolled gridding and forcing of gridded values to the value of one (i.e., no calibration as distance from a well exceeds a certain limit) were attempted (Figure 10). Geological consideration may be added to the gridding through the use of fault, terrane or basin boundary maps to guide how calibration coefficients are interpolated and extrapolated. For example, calibration coefficients calculated within the Abrolhos Sub-Basin could be treated separately from those calculated in the Houtman Sub-Basin. This would ensure that differences in the tectnostratigraphic evolution of the two sub-basins do not interfere in the depth calibration process.

If this velocity analysis and depth conversion methodology were to be applied to a smaller area, it may prove beneficial to create a 3D velocity model for use in depth conversion, rather than a series of 2D velocity models along seismic lines. More advanced gridding methods such as co-kriging could be used to integrate well and seismic velocities (e.g. Dubrele, 2003) to create this 3D velocity model. The integration of well and stacking velocities together using the co-kriging process would negate the need to calibrate the depth converted horizons. Alternatively, should a 3D seismic survey (with 3D seismic stacking velocity dataset) be available then the given methodology could be applied to calibrate this 3D distribution of stacking velocities to well velocities. Buland et al. (2011) describe a method where Bayesian statistics are employed to create a smoothly-distributed 3D velocity model using stacking velocities. The method presented by Buland et al., (2011) is a modified Dix inversion constrained by a prior understanding of the geology, i.e. well velocity logs integrated with the stacking velocities. This method could be integrated with the approach presented here to create a smooth 3D velocity model that is calibrated against well velocities.

Conclusion

A methodology for calibrating seismic stacking velocities against well velocities for use in the depth conversion of seismic interpretations has been developed. The calibration of stacking velocities against well velocities in the northern Perth Basin has been shown to decrease uncertainty in the depth conversion of seismic interpretation when using seismic stacking velocities. Examples have shown that these depth conversion errors are reduced to a level that will produce less than ±20 gu errors when used as constraints in gravity modelling. Future work considered includes how to apply this methodology to smaller survey areas, e.g. 3D seismic surveys, and how to incorporate geological understanding into the calibration coefficient workflow.

Acknowledgements

We thank Andrea Cortese, Ron Hackney and Nadege Rollet for reviewing the document and Theo Chiotis for drafting the figures. This document is published with permission of the Chief Executive Officer of Geoscience Australia.

References

Akima, H., 1970. A new method of interpolation and smooth curve fitting based on local procedures. Journal of the ACM, 17(4), p. 589-602.

Al-Chalabi, M., 1974. An analysis of stacking, RMS, average and interval velocities over a horizontally layered ground. Geophysical Prospecting, Vol. 22, No. 3, p. 458-475.

Buland, A., Kolbjornsen, O, and Carter, A.J., 2011. Bayesian Dix inversion. Geophysics, Vol. 76, No. 2, p. R15-R22.

Dix, C.H., 1955. Seismic velocities from surface measurements. Geophysics, Vol. 20, p. 68-86.

Dubrele, O., 2003. Geostatistics for seismic data integration in earth models. 2003 Distinguished Instructor Short Course, European Association of Geoscientists and Engineers.

Etris, E.L., Crabtree, N.J., Dewar, J., and Pickford, S. 2001. True depth conversion: more than a pretty picture. CSEG Recorder, November, p. 11-22.

Japsen, P., 1993. Influence of lithology and Neogene uplift on seismic velocities in Denmark: implications for depth conversion of maps. American Association of Petroleum Geologists Bulletin, Vol. 77, No. 2, p. 194-211.

Jones, A.T., Kennard, J.M., Nicholson, C.J., Bernardel, G., Mantle, D., Grosjean, E., Boreham, C.J., Jorgensen, D.C. and Robertson, D., 2011. New exploration opportunities in the offshore northern Perth Basin. APPEA Journal, 51, 45–78.

Mjelde, R., Raum, T., Murai, Y., and Takanami, T., 2007. Continent-ocean-transitions: Review, and a new tectono-magmatic model of the Vøring Plateau, NE Atlantic, Journal of Geodynamics, Vol. 43, p. 374-392.

Mory, A.J. and Iasky, R.P., 1996. Stratigraphy and structure of the onshore northern Perth Basin, Western Australia. Western Australia Geological Survey, Report 46. 99p.

Norvick, M.S., 2004, Tectonic and stratigraphic history of the Perth Basin, Record 2004/16, Geoscience Australia: Canberra.

Petkovic, P., 2004. Time-depth functions for the Otway Basin. Geoscience Australia Record 2004/02. 43p.

Pfahl, M., 2011. Tectonic subsidence, thermal history and petroleum system modelling of the offshore northern Perth Basin. Unpublished BSc Honours dissertation, Australia School of Petroleum, University of Adelaide.

Quaife, R., Rosser, J. and Pagnozzi, S., 1994, The structural architecture and stratigraphy of the offshore northern Perth Basin, in Purcell, P.G. and Purcell, R.R. (Eds), The Sedimentary Basins of Western Australia: Proceedings of the Petroleum Exploration Society of Australia Symposium, Perth, p. 811–822.

Reilly, J.M., 1993. Integration of well and seismic data for 3D velocity model building. First Break, Vol. 11, No. 6, p. 247-260.

Rider, M.H., 1986. The geological interpretation of well logs. Blackie and Son Limited. 175p.

Tsvankin, I., 2005. Seismic signatures and analysis of reflection data in anisotropic media. Elsevier Science Publishing Co.

Veeken, P., Filbrandt, J., and Al Rawahy, M., 2005. Regional time-depth conversion of the Natih E horizon in Northern Oman using seismic stacking velocities. First Break, Vol. 23, p. 35-45.

White R.S., Smith, L.K., Roberts, A.W., Christie, P.A.F., Kusznir, N.J. & iSIMM Team, 2008. Lower-crustal intrusion on the North Atlantic continental margin, Nature, Vol. 452, p. 460–464.

Appendix A – Extracting data

EXTRACTING VELOCITY INFORMATION FROM GEOFRAME

Sonic log

Sonic log data can be exported from GeoFrame by the following method:

1. Log in to a GeoFrame project
2. Click the 'Data' button
3. Goto 'Loaders and Unloaders' then 'Data Save'. Start a new run.
4. Click the magnifying glass button to 'bring up a quickie data focus to select data'.
5. Show 'Borehole'
6. Navigate to the necessary borehole, click on it and press 'Expand' (or alternatively, click on the borehole and show 'Activity'.
7. Navigate to the sonic log (or other borehole log) and click on it. Press 'Ok'.
8. Ensure that the destination is set to File, with format as ASCII, and select the output file name and location. Make sure that the control file is set to a LAS format.
9. Press .Run'.
10. Navigate to the directory as set in step 8 to find your sonic log.

Checkshot

Checkshot data can be exported from GeoFrame by the following method

1. Open GeoFrame
2. Login to project
3. Open Application Manager
4. Open 'Data' from 'Managers
5. From 'Data Managers' open 'General'
6. Right click on the project, select 'Expand By Type' then 'Field'
7. Right click on the appropriate 'Field', select 'Expand By Type' then 'Well'.
8. Right click on a well, select 'Expand By Type' then 'Borehole
9. Right click on a borehole, select 'Expand By Type' then 'Well Checkshot Survey
10. Double click on the pertinent velocity survey (i.e. Well Name – Velocity Survey – Checkshot).
11. Click on the 'Display arrays in the well checkshot survey in table format' button
12. Select 'File Only' as the Destination. Click the 'File Selection' button to choose an output location and file name. Click 'Run' to export the data.

Appendix B - Depth conversion process in Petrosys

This is an outline of the depth conversion process in Petrosys, including loading of data (lines, interpretation, and velocities), application of Dix equation, depth conversion, grid multiplication, application of calibration coefficient etc.

1. Create new seismic data file (SDF)
    a. Petrosys Mapping -> New
    b. Enter the location and name of the SDF file, and names of horizons to be loaded
2. Load seismic lines
    a. Import -> Geoquest -> IESX-GF4.5-direct
    b. Select project, SDF file to load data to and seismic lines to load
    c. Load selected line coordinates to sdf… -> use easting and northing coordinates
3. Load interpretation
    a. From above, select horizons to import from the 'Horizons' tab
    b. Load horizon data to sdf… -> match the Geoframe horizon to the Petrosys horizon
4. Load stacking velocities
    a. Petrosys Mapping -> Import -> Velocities -> Western
    b. Ensure that your data is in the Western Geophysical format and that the names of the seismic lines in the velocity file conform to those in the Petrosys SDF.
5. Depth convert water bottom
    a. Petrosys Mapping -> Functions -> Single-Formula
    b. In the left hand text box enter: DEPTH[wb]
    c. In the right hand text box enter: TWT[wb] / 2000 * 1500
    d. Where wb is the name of the water bottom horizon
6. Calculate interval velocities
    a. Petrosys Mapping -> Velocities/Depth -> Velocities -> Compute from stacking velocities
    b. Computation method: Interval velocity from stacking using Dix
    c. Horizon 1: Water Bottom (initially), horizon 2:horizon below water bottom
7. Depth convert using interval velocities
    a. Petrosys Mapping -> Velocities/Depth -> Depth convert -> Interval velocities…
    b. Depth convery using: Interval velocity profile
    c. Ensure that the horizons are those for which interval velocities are already calculated
8. Multiply depths by calibration coefficient grid
    a. Petrosys Mapping -> Functions -> Function-Lists -> Edit -> Create
    b. In the function code text box enter: d = d*c;
    c. Press 'Validate function code', then 'Update from code'
    d. Assign the 'd' variable type to 'Seismic Line', overwrite mode to 'Replace exisiting', data type to 'Depth' and horizon 1 to a depth converted horizon.
    e. Assign the 'c' variable to 'Petrosys grid', and choose the calibration coefficient grid.
    f. Press 'Ok'